Decreased Expression of Peroxiredoxins in Fuchs' Endothelial Dystrophy

Ula V. Jurkunas,[1,2,3] *Ian Rawe,*[1] *Maya S. Bitar,*[1,3] *Cheng Zhu,*[1,3] *Deshea L. Harris,*[1,3] *Kathryn Colby,*[1,2,3] *and Nancy C. Joyce*[1,3]

Purpose. To compare the relative expression of peroxiredoxin (Prx) proteins in normal human corneal endothelium with endothelium in corneas affected by Fuchs' endothelial dystrophy (FED) and between normal human endothelium and epithelial/stromal tissue.

Methods. Human corneal endothelial cell-Descemet's membrane (HCEC-DM) complexes from normal and FED corneal buttons were dissected from the epithelium/stroma. For proteomic analysis, HCEC-DM protein extracts were separated by using two-dimensional gel electrophoresis. Relative differences in protein spot density was analyzed. Proteins of interest, including Prx isoforms, were identified by MALDI-TOF (matrix-assisted desorption ionization-time of flight) mass spectrometry. Western blot analysis compared the relative expression of Prx isoforms in normal and FED endothelium and between normal endothelium and normal epithelium/stroma. Expression of Prx-2 mRNA was compared by using real-time PCR.

Results. Proteomic analysis identified differences in the relative expression of Prx isoforms between normal and FED endothelium. Western blot analysis confirmed that expression of Prx-2, −3, and −5 was significantly decreased ($P < 0.05$) in FED cells. Normal HCECs expressed significantly ($P < 0.05$) higher levels of Prx-2 and −3 than did the epithelium/stroma. Expression of Prx-5 was not significantly different ($P > 0.05$) in the endothelium versus the epithelium/stroma. Real-time PCR analysis revealed that Prx-2 mRNA was significantly decreased ($P = 0.027$) in FED samples.

Conclusions. Prx proteins were identified in human corneal endothelium. The fact that Prx-2 and −3 were expressed at significantly higher levels in HCEC-DM compared with the epithelium/stroma reflects the different physiologic activities of individual corneal cell types. Significantly decreased expression of Prx-2, −3, and −5 in FED may suggest an alteration in the ability of endothelial cells to withstand oxidant-induced damage and may be closely related to the pathogenesis of this disease. (*Invest Ophthalmol Vis Sci.* 2008;49:2956–2963) DOI: 10.1167/iovs.07-1529

From the [1]Schepens Eye Research Institute, Boston, Massachusetts; the [2]Massachusetts Eye and Ear Infirmary, Boston, Massachusetts; and the [3]Department of Ophthalmology, Harvard Medical School, Boston, Massachusetts.

Supported by National Eye Institute Grant K12 EY016335 (UVJ), the New England Corneal Transplant Research Fund (KC), the Joint Clinical Research Center, Massachusetts Eye and Ear Infirmary, and Schepens Eye Research Institute (KC, NCJ).

Submitted for publication November 29, 2007; revised February 14, 2008; accepted May 12, 2008.

Disclosure: **U.V. Jurkunas**, None; **I. Rawe**, None; **M.S. Bitar**, None; **C. Zhu**, None; **D.L. Harris**, None; **K. Colby**, None; **N.C. Joyce**, None

The publication costs of this article were defrayed in part by page charge payment. This article must therefore be marked "*advertisement*" in accordance with 18 U.S.C. §1734 solely to indicate this fact.

Corresponding author: Ula V. Jurkunas, Massachusetts Eye and Ear Infirmary, 243 Charles Street, Boston, MA 02114; ula_jurkunas@meei.harvard.edu.

Fuchs' endothelial dystrophy (FED) is the most common cause of endogenous endothelial dysfunction and is the third most common indication for corneal transplantation in the United States.[1] Even though this dystrophy was first described more than 100 years ago, the primary etiology of the endothelial cell degeneration is not yet known.[2] In early stages, the dystrophy manifests by the formation of corneal guttae or dysregulated deposition of wide-spaced collagen between human corneal endothelial cells (HCECs) and Descemet's membrane (DM), with concomitant changes in HCEC shape, size, and density.[3–5] Excessive deposition of collagen VIII has been noted in FED Descemet's membrane, and mutations in collagen VIII have been identified in familial, early-onset FED.[6] In the later stages of the disease, the progressive loss of Na^+-K^+-ATPase pump sites is associated with the inability of the endothelium to maintain corneal deturgescence, leading to corneal edema.[7]

Recently, nuclear labeling and mRNA analysis techniques showed that FED endothelial cell death occurs via apoptosis.[8–10] In other organ systems where cellular apoptosis is accompanied by abnormal extracellular matrix deposition, such as amyloid plaques in Alzheimer's disease or drusen in age-related macular degeneration, a strong causal factor in cell death is oxidative stress due to excessive generation of reactive oxygen species (ROS).[11] There is mounting evidence that oxidative stress induces damage to corneal endothelium in FED.[12] Previous studies by Buddi et al.[13] evaluated the relative amounts of cytotoxic byproducts of ROS in FED corneas. Although most of the differences between normal and FED were noted in the corneal epithelium, increased amounts of nitrotyrosine, an ROS byproduct, were also noted in the FED endothelium. From the genetic standpoint, Gottsch et al.[14] found decreased transcript levels of the anti-oxidant glutathione *S*-transferase-pi in FED via serial analysis of gene expression.

In initial studies from our laboratory, 2-D gel electrophoresis, MALDI-TOF protein identification, and Western blot analysis were used to compare protein expression between FED and normal corneal endothelium. This analysis revealed several protein differences, one of which was marked overexpression of clusterin in FED endothelium.[15] Clusterin is a protein that protects against oxidative stress-induced cellular apoptosis. The current studies have further investigated the differential expression of proteins in FED with a particular focus on proteins with antioxidant properties. Specifically, MALDI-TOF analysis of normal gels at a 15- to 30-kDa range (isoelectric point [pI], 6.0–9.0) identified the expression of a novel class of antioxidants, peroxiredoxins (Prx). We then investigated whether there is a difference in expression patterns of Prx between normal and FED endothelial specimens. In the previous 2-D gel studies, proteins were separated in the first dimension by using a linear pH 3 to 10 gradient. In the current studies, we changed the technique of isoelectric focusing by employing nonlinear gradient IPG strips to expand the region of the gel around neutral pH, thus promoting better separation of proteins that have pIs in this area.

Prx functions by removing cellular hydrogen peroxide. Six isotypes of Prx (1–6) have been identified in mammals. The subfamily of Prx 1 to 4 contains two conserved active site cysteine (Cys) residues that use thioredoxin as an intermediate electron

Investigative Ophthalmology & Visual Science, July 2008, Vol. 49, No. 7

donor. Prx-5 also has two conserved active Cys residues, but does not possess a 40-amino-acid residue segment on the C terminus and is the smallest isoform. Prx-6 contains only one conserved Cys residue.[16–18] Since different isoforms of Prx proteins have different cellular functions, we compared the relative expression of Prx isoforms in normal and FED endothelium by both software analysis of 2-D gel patterns and by Western blot analysis. Real-time PCR was used to confirm the proteomic results by comparing the relative mRNA levels of Prx-2 between the normal and diseased HCECs. We also used Western blot analysis to compare the relative expression of Prx isoforms in normal corneal endothelium and in epithelial/stromal tissues.

Materials and Methods

Human Tissue

Donor confidentiality was maintained according to the Declaration of Helsinki. The study was approved by the Massachusetts Eye and Ear Institutional Review Board. Informed consent was obtained from patients undergoing corneal transplantation for FED. After surgical removal of the FED corneal buttons, they were placed in cornea preservation medium (Optisol-GS; Bausch & Lomb, Rochester, NY) at 4°C. Two thirds of the FED corneal button was used for the study and one third was used for histopathologic confirmation of the diagnosis. Normal human corneal buttons were obtained from the New England Tissue Bank (Boston, MA) and the National Disease Research Interchange (Philadelphia, PA) and were used as the control. We used our previously published criteria for obtaining normal control corneas from the tissue banks. These criteria include using corneas with endothelial cell counts ≥1500.[19] All normal corneas used in the study were considered to be unsuitable for transplantation because of the lack of blood samples from the donor for serology tests, peripheral scars or infiltrates, pterygia, or donor age. In accepting the corneas, the overall health of the donor before death was considered, and tissue was rejected from donors with a history that indicated possible damage to the endothelium. Corneas were not accepted for study if there were too long a period (>24 hours) between time of death and time of preservation, corneal guttae, or any endothelial abnormality seen on the specular biomicroscopy; corneas from donors with glaucoma, sepsis, or ocular infection; or corneas from donors who were on large doses of chemotherapeutic agents. Since normal corneal buttons were stored in preservative before sample preparation, the FED corneas were also kept in the preservative, to negate any effects of storage conditions on protein expression.

Sample Preparation

Table 1 presents information regarding the tissue samples used in these studies. Samples were prepared by pooling donor tissue during the protein extraction step. Human corneal buttons were recovered from the preservative and briefly rinsed in PBS. Under a dissecting microscope Descemet's membrane, along with the endothelial cell layer (HCEC-DM complex) was dissected from the cornea and placed into an ultracentrifuge tube. The HCEC-DM complex was washed with 10 mM HEPES (pH 7.4 buffer), before protein extraction. Samples used for 2-D gel electrophoresis were subjected to an extra washing step with HEPES buffer (10 mM, pH 7.4) followed by centrifugation at 5000 rpm for 10 minutes. Protein extraction buffer ER3 (Bio-Rad, Hercules, CA) containing 5 M urea, 2 M thiourea, 2% CHAPS, 2% SB 3-10, 40 mM Tris, 0.2% 3:10 ampholyte (Bio-Lyte; Bio-Rad), and 1 mM tributyl phosphine (TBP) was added to the HCEC-DM sample. Samples were solubilized by pipetting up and down, followed by incubating the tissue at room temperature for 30 minutes. Solubilized protein was recovered by ultracentrifugation of samples at 40,000 rpm, 21°C for 1 hour.

Table 1. Donor Information

Pooled Sample	FED HCEC-DM* Age	FED HCEC-DM* Sex	Normal HCEC-DM and/or Stroma/Epithelium Age	Normal HCEC-DM and/or Stroma/Epithelium Sex	Death-to-Preservation Time (h)†	Use of Samples
1			77	M	5.8	2-D gel
			78	M	17	
2			57	F	21	
			62	M	18	
			53	F	20	
3	54	M	62	F	12	
	66	F	69	M	17	
	64	F				
	72	F				
4	85	M	52	M	20	Western blot analysis
	73	M	64	F	23	
	49	F	80	M	6	
	77	M				
	62	F				
5	59	F	53	F	19	
	67	F	64	F	19	
6	85	M	80	M	6	
	73	M	64	F	19	
	49	F	53	F	19	
7	77	M	80	M	6	
	62	F	64	F	19	
			53	F	19	
8	81	F	72	F	10	
	67	M	67	F	11	
9	69	M	72	F	10	
	66	F	67	F	11	
10	85	F	72	F	10	
	81	F	67	F	11	
	69	M				
11			64	M	21	
			63	M	12	
			62	F	19	
12			67	M	24	
			69	M	20	
			57	M	21	
			54	F	23	
13			50	F	3	
			50	M	19	
14			52	M	20	
			64	F	23	
			80	M	6	
15	57	F	70	F	8	Real-time PCR
	78	M	70	F	5	
	81	M	67	F	12	
	63	M				
16	82	F	72	M	9	
	50	F				
	51	F				
17	69	F	72	M	9	
	72	M	74	F	16	
18	61	F	56	F	19	

FED, Fuchs' endothelial dystrophy; HCEC-DM, human corneal endothelium and Descemet's membrane.

* FED specimens taken during keratoplasty were placed in Optisol-GS at 4°C.

† Time (hours) between death and placement of the cornea in Optisol-GS at 4°C.

HCEC-DM protein samples were used for 2-D gel electrophoresis and Western blot analysis. For some studies, the remaining corneal stroma and epithelium were cut into small pieces and homogenized. Protein

was extracted with ER3 extraction buffer in the same manner as used for HCEC-DM protein sample preparation. Protein concentration of the samples was determined by modified protein assay (Bio-Rad).

2D-Gel Electrophoresis

Equal amounts of protein (Table 1, samples 1–3) were loaded onto immobilized pH 3 to 10, nonlinear gradient, 17 cm IPG strips (Bio-Rad) for passive rehydration over 14 hours. The use of a nonlinear IPG strip expanded protein separation at a pI close to pH 7.0. Isoelectric focusing was performed (Protean IEF Cell; Bio-Rad) with a gradual voltage increase up to 10,000 volts for a total of 60,000 volt-hours. Second-dimensional separation was performed using 8% to 16% precast gradient poly-acrylamide gels (BioRad). Gels (193 × 183 × 1.0 mm) were run at 350 volts until the bromophenol blue dye disappeared. Gels were then fixed in 10% methanol and 7% acetic acid, stained overnight (SYPRO Ruby; Invitrogen, Carlsbad, CA), and washed in water for 1 hour before imaging.

Gel Image Capture and Analysis

Protein spots were imaged (ProExpress Proteomic Imaging system; PerkinElmer, Boston, MA) with optimized excitation (480/80 nm) and emission (650/150 nm) filters for the gel stain (Sypro Ruby Protein Gel Stain; Invitrogen). Gel images were analyzed (Automatic Analysis Wizard setting in the ProFinder software; Perkin-Elmer/Nonlinear Dynamics, Newcastle-upon-Tyne, UK). Relative differences in the normalized volume of each protein spot were compared between two pooled samples from normal HCEC-DM and then between pooled samples from normal and FED HCEC-DM. Protein spots of interest were chosen from the gel spot-picking robot (ProXcision; PerkinElmer) equipped with a CCD camera and filter sets for the stain (Sypro Ruby; Invitrogen).

MALDI-TOF Identification of Protein Spots

Gel pieces were placed in a plate (ZipPlate; Millipore, Billerica, MA) and processed as described in the manufacturer's protocol. In brief, the gel plug was washed in 25 mM ammonium bicarbonate/5% acetonitrile for 30 minutes and destained with ammonium bicarbonate/50% acetonitrile two times for 30 minutes each. Gel plugs were then dehydrated with 100% acetonitrile for 15 minutes, rehydrated in 15 μL of 25 mM ammonium bicarbonate containing 100 ng trypsin gold (Promega, Madison, WI), and then incubated at 30°C overnight. The C_{18} resin (ZipPlate; Millipore) was then activated with 9 μL acetonitrile for 15 minutes at 37°C. Peptides were washed out of the gel plug with 180 μL 0.1% trifluoroacetic acid (TFA) for 30 minutes and then bound to the C_{18} resin by low vacuum followed by washing twice with 100 μL TFA in a high vacuum. The peptides were then directly eluted onto a disposable MALDI (matrix-assisted desorption ionization) target plate (PerkinElmer) by direct vacuum elution with matrix α-cyano-4-hydroxy cinnamic acid (α-CHCA at 10 mg/mL; LaserBiolabs, Sophid-Antipolis, France) in 50% acetonitrile/50% TFA. Matrix was air dried, allowing crystals to form. The MALDI plate was then loaded (prO-TOF 2000 MALDI-TOF; PerkinElmer). The instrument was calibrated using a two-point calibration method from a peptide calibration mix (LaserBiolabs). Sample data were acquired with a mass range of 750 to 4500 Da. Proteins were identified by searching a local copy of the NCBI (National Center for Biotechnology Information, www.ncbi.nih.gov) protein database (ProFound search engine; Rockefeller University, New York, NY).

Western Blot Analysis

Equal amounts of protein from normal HCEC-DM and FED specimens (Table 1; samples 4–10) or from normal HCEC-DM and epithelium/stroma samples (Table 1; samples 11–14) were loaded on 10% Bis-Tris gels for SDS-PAGE. Positive controls consisted of cell lysate (LNCap; Upstate Cell Signaling, Lake Placid, NY) for identification of Prx-2 and HeLa cell lysate (Santa Cruz Biotechnology, Santa Cruz, CA) for identification of Prx-3 and −5. Peptides were then electrophoretically transferred to a polyvinylidene difluoride (PVDF) membrane (Millipore, Bedford, MA), and nonspecific binding was blocked by incubation for 1 hour at room temperature in 5% nonfat milk diluted in PBS. Membranes were incubated overnight at 4°C with rabbit polyclonal anti-Prx-2 diluted 1:1000 (Upstate Cell Signaling), mouse monoclonal anti-Prx-3 (LabFrontier, Seoul, Korea) diluted 1:600, and mouse monoclonal anti-Prx-5 (LabFrontier) diluted 1:500, rabbit polyclonal anti-superoxide dismutase-1 (SOD-1) diluted 1:100 (Santa Cruz Biotechnology), mouse monoclonal anti-vimentin diluted 1:300 (Santa Cruz Biotechnology), or mouse monoclonal anti-β-actin diluted 1:6000 (Sigma-Aldrich, St. Louis, MO). All dilutions were made in blocking solution. Blots were rinsed, reblocked, and exposed for 1 hour to horseradish peroxidase (HRP)-conjugated donkey anti-mouse IgG for Prx −3 and −5, β-actin, and vimentin blots (Jackson ImmunoResearch Laboratories, Inc., West Grove, PA) and anti-rabbit IgG for Prx-2 and SOD-1 blots. All secondary antibodies were obtained from Jackson ImmunoResearch Laboratories, Inc. and diluted in 1:2000 in blocking solution. After washing in 0.1% Triton X-100, peptides were detected with a chemiluminescent substrate (SuperSignal, Rockford, IL). Images were digitally scanned and analyzed with NIH Image software version 1.61 (available by ftp at http://rsb.info.nih.gov/nih-image developed by Wayne Rasband and provided in the public domain by the National Center for Biotechnology Information, Bethesda, MD). Protein content was normalized according to β-actin content. Experiments were repeated at least two times. Results were averaged and the standard error was calculated. Statistical analysis using Student's unpaired *t*-test was performed with commercial software (Excel 2002; Windows XP; Microsoft, Redmond, WA). $P < 0.05$ was considered to be significant.

Real-Time PCR

Total RNA was extracted from normal and FED HCEC-DM complexes (Table 1, samples 15–18) as recommended by the manufacturer (TRIzol; Invitrogen). Samples were purified from DNA contamination by treating them with DNase I (DNase I, Amplification Grade; Invitrogen). RNA quantity and quality were assessed by spectrophotometric analysis. For all samples, cDNA was prepared by reverse transcription from equal amounts of RNA in a volume of 40 μL using a commercially available kit (Promega). Relative expression levels of Prx-2 were assessed by real-time PCR using a sequence-detection system instrument (Prism 7900 HT; Applied Biosystems [ABI], Foster, CA). Primers and probes for Prx-2 (*Taq*Man Gene Expression Assays, inventoried) and for the endogenous control β_2-microglobulin (β_2-MG)[15] (human B2M endogenous control, FAM/MGB probe, *Taq*Man Endogenous Controls) were obtained from Applied Biosystems. Samples ($n = 4$) were assayed in duplicate in a total volume of 50 μL, using thermal cycling conditions of 10 minutes at 95°C followed by 50 cycles of 95°C for 15 seconds and 60°C for 1 minute. No template controls were run in each assay to confirm lack of DNA contamination in reagents used for amplification. For data analysis, the comparative threshold cycle (C_T) method was adopted with the relative mRNA levels in normal subjects selected as the calibrator. The C_T was set in the exponential phase of the amplification plot. To normalize the amount of target gene in each sample, we calculated the difference in C_T (ΔC_T) by subtracting the average C_T of the endogenous control from that of the target gene. The $\Delta\Delta C_T$ was calculated by subtracting the ΔC_T of FED samples from the mean value of the ΔC_T of normal samples. The amount of mRNA for Prx-2 in FED was expressed relative to the amount present in the calibrator, using the formula $2^{-\Delta\Delta C_T}$. Results were averaged and the SEM was calculated. Statistical analysis was performed with Student's unpaired *t*-test (Excel 2002 for Windows XP; Microsoft). $P < 0.05$ was considered to be significant.

Results

Proteomic Analysis of Prx Isoform Expression in FED and Normal HCEC-DM

Two-dimensional gel proteomic analysis was chosen as a means to identify differences in protein expression between

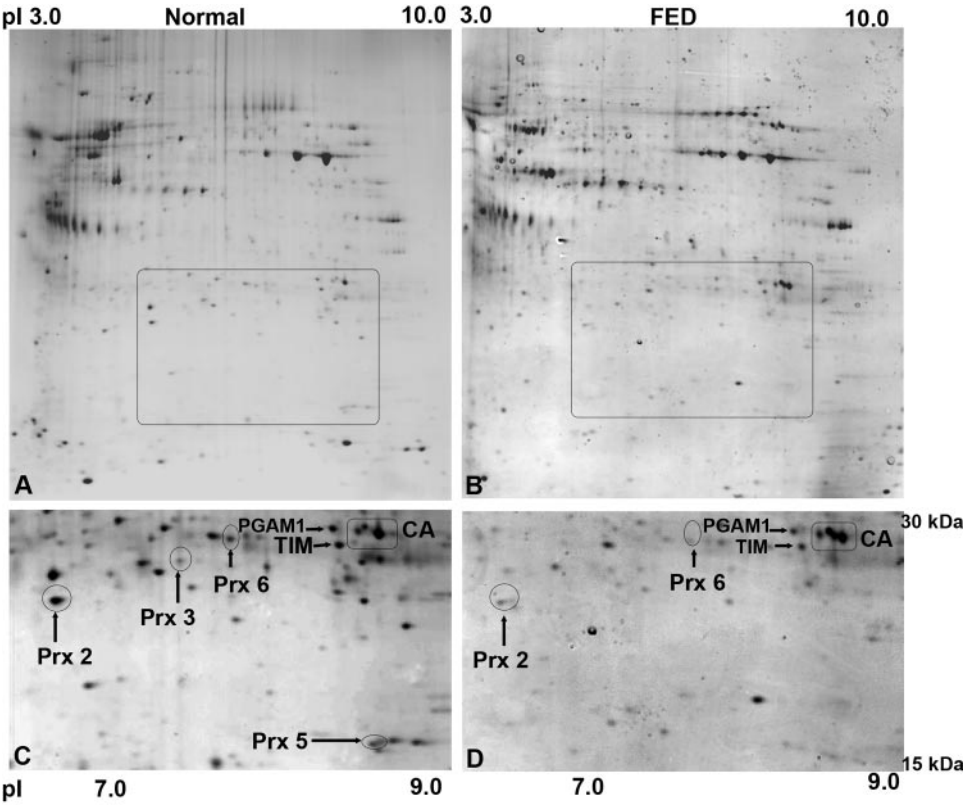

FIGURE 1. Representative 2-D maps of HCEC-DM proteins pooled from normal and FED donors. Complete maps of ruby–stained protein spots are shown for the pooled normal sample (**A**) and the pooled FED sample (**B**). Outlined regions in both (**A**) and (**B**) show areas of interest which are shown enlarged in (**C**) and (**D**), respectively. The position of Prx isoforms −2, −3, −5, and −6; phosphoglycerate mutase-1 (PGAM1); triosephosphate isomerase (TIM); and carbonic anhydrase-III (CA) are indicated. The relative intensity of the protein spots for Prx-2 and −6 in (**D**) were lighter than the corresponding spots in (**C**). Spots corresponding to Prx-3 and −5 in (**C**) were not detectable in (**D**).

the endothelium of FED and normal donors that might reflect important physiological changes that occur in FED endothelial cells. Before conducting these studies, a preliminary study was performed to determine the reproducibility of 2-D gel-based protein separation using a nonlinear pH 3 to 10 gradient in the first dimension. For these studies, HCEC-DM complexes were isolated from the corneas of normal donors ranging in age from 53 to 78 years. Proteins were extracted, pooled to form two independent samples (Table 1; pooled sample 1 and 2), and then separated on two-dimensional gels. The resultant 2-D images from the two pooled samples were compared by software analysis. Results showed a very similar pattern of stained (Sypro Ruby; Invitrogen) protein spots, indicating the reproducibility of the separation technique (data not shown).

Once it was determined that the protein pattern was reproducible on 2-D gels, a study was conducted to compare the pattern of HCEC-DM complexes isolated from FED and normal donors. Proteins were extracted from HCEC-DM complexes isolated from four FED corneas and corneas from two decade-matched normal control subjects. Extracts were pooled to form one FED and one normal sample (Table 1, pooled sample 3), and proteins were separated on 2-D gels as previously. The pattern obtained from the pooled sample prepared from normal donors is shown in Figure 1A, and the pattern of the pooled sample from the FED donors is in Figure 1B. An area of particular interest on the 2-D gels was located within an approximate pH range of 6.0 to 9.0, and a relative molecular weight range of 15 to 30 kDa. This area is outlined on the gel images in Figures 1A and 1B and enlarged in Figures 1C and 1D. Within this area of the gels was a group of protein spots that showed similar normalized volumes. MALDI-TOF analysis identified these spots as phosphoglycerate mutase-1 (PGAM-1), triosephosphate isomerase (TIM), and carbonic anhydrase-III (CA-III; Table 2). These spots are identified in Figures 1C and 1D. Additional protein spots were observed in this region of the gel prepared from the normal control samples. Among the proteins that had a known match in the general proteomic database were Prx-2, −3, −5, and −6 (Table 2). Comparison of the normalized volume of these spots showed that expression of Prx-2 in the pooled sample from the normal control samples was 5.033 times higher than in the FED sample. Spots corresponding to Prx-3 and −5 were detected in the normal control sample, but not in the FED sample. The normalized volume of Prx-6 was detected 4.059 times higher in normal control samples.

Western Blot Comparison of Prx Isoform Expression in Normal and FED HCEC-DM

Western blot analysis was next performed to verify the differential expression of Prx-2, −3, and −5 in normal and FED

TABLE 2. Identification of Proteins by MALDI-TOF

Protein	Molecular Mass (kDa)	Accession No.	Probability*
Prx 2	22.1	P32119	1.13E-005
Prx 3	27.7	P30048	3.65E-005
Prx 5	16.9	P30044	3.18E-020
Prx 6	25.0	P30041	1.00E-016
PGAM 1	28.9	P18669	6.13E-003
TIM	26.8	P60174	4.17E-005
CA III	29.8	P07451	5.12E-005

Proteins were separated on 2-D gels and identified by MALDI-TOF following digestion. All identified proteins are available in the SWISS-PROT database via the accession number. Prx, peroxiredoxin; PGAM1, phosphoglycerate mutase 1; TIM, triosephosphate isomerase; CA III, carbonic anhydrase III.

* E of 003 and greater is a positive match.

HCEC-DM that was indicated by the previous 2-D gel software analysis. The expression of Prx-6 was not pursued by Western blot analysis due to the inability to find an antibody that worked consistently in Western blot analysis. β-Actin was used for normalization of protein load. Figure 2A presents a representative Western blot and Figure 2B presents the densitometric analysis of data averaged from seven independent samples (Table 1, pooled samples 4–10). HCEC-DM from FED donors showed a statistically significant decrease in all three Prx isoforms compared with normal, decade-matched donors (Prx-2: $P = 0.0045$; Prx-3: $P = 0.0080$; and Prx-5: $P = 0.011$).

Expression of SOD-1 and Vimentin in Normal and FED HCEC-DM

To assess whether downregulation of Prx isoforms in FED is specific, the relative expression of vimentin, an intermediate filament protein, and the antioxidant enzyme, superoxide dismutase (SOD)-1, were compared between normal and FED HCEC-DM samples (Table 1, pooled samples 9 and 10). Figure 3A presents a representative Western blot, whereas Figure 3B provides densitometric data indicating that relative levels of vimentin and SOD-1 were not significantly different ($P > 0.05$) between FED and normal samples.

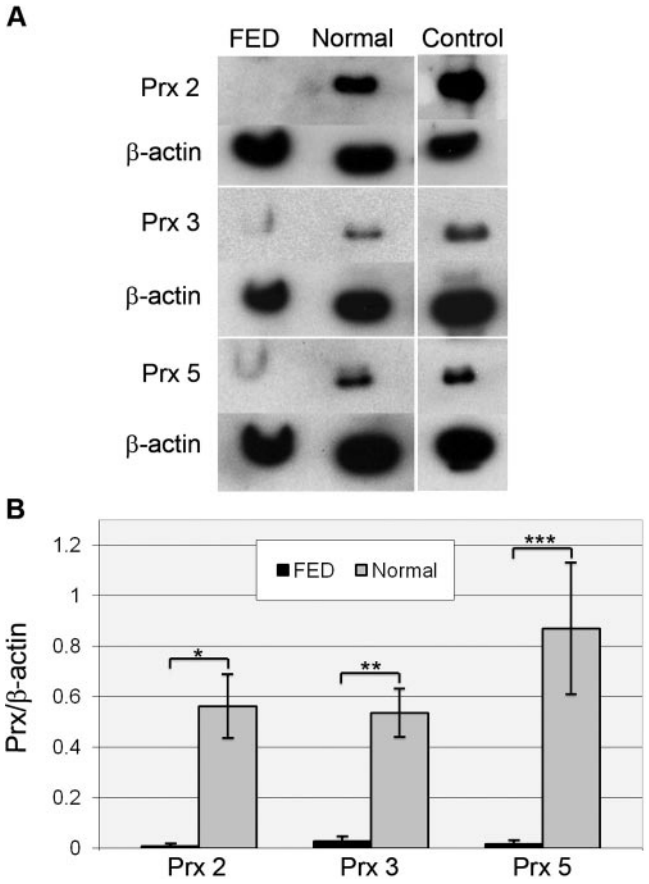

FIGURE 2. Western blot analysis of Prx isoform expression in normal and FED HCEC-DM complexes. (**A**) Representative Western blot analysis comparing the expression of Prx-2, −3, and −5 in FED and normal corneal endothelial samples. Positive controls included LNCap cell lysate for Prx-2 and HeLa cell lysate for Prx-3 and −5. β-Actin was used for normalization of protein loading. (**B**) Densitometric comparison of the average expression of Prx-2, −3, and −5. Bars: SEM. *$P = 0.0045$; **$P = 0.0080$; ***$P = 0.011$.

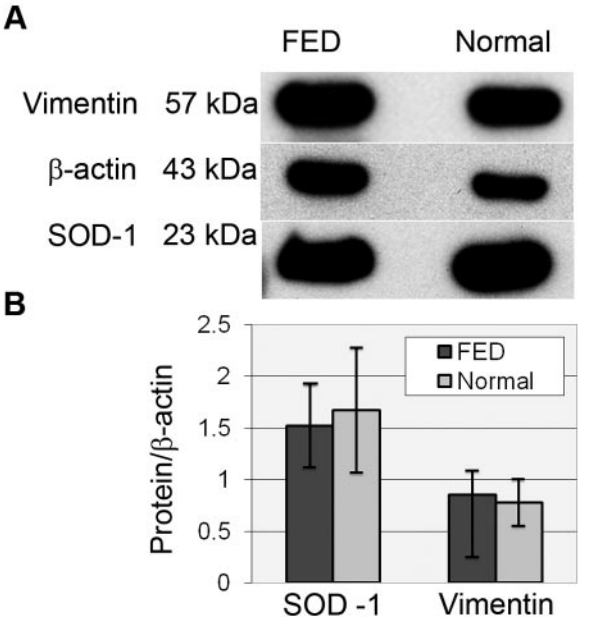

FIGURE 3. Western blot comparison of vimentin and SOD-1 expression in HCEC-DM complexes from FED and normal donors. (**A**) Representative Western blot analysis for vimentin and SOD-1. β-Actin was used for normalization of protein loading. (**B**) Averaged densitometric data showed no significant difference in the relative expression of these proteins. Bars: SEM.

Western Blot Comparison of Prx Isoform Expression in Normal HCEC-DM and in Epithelium/Stroma

Since Prx proteins have not been identified in human cornea, we investigated whether Prx expression is specific to corneal endothelium or is present in the other corneal layers. Semiquantitative Western blot analysis was performed to compare the expression of Prx isoforms in normal human corneal endothelium to epithelium/stroma. For this analysis, protein was extracted from HCEC-DM complexes and from the remaining epithelial/stromal tissue from normal donors aged 50 to 80 years. Extracts were pooled to yield four independent samples (Table 1, pooled samples 11 to 14). Figure 4A presents representative Western blot images comparing the expression of Prx-2, −3, and −5 in normal corneal endothelium and in the epithelium/stroma. Figure 4B presents the densitometric analysis using β-actin for normalization. The average expression of Prx-2 was 30-fold higher in HCEC-DM than in epithelium/stroma ($P = 0.0034$). Prx-3 expression was not detectable in samples prepared from the epithelium/stroma ($P = 0.00062$). Prx-5 was detected in epithelial/stromal samples, but was not significantly different from that of HCEC-DM ($P = 0.5$).

Real-Time PCR Comparing Prx-2 Expression between Normal and FED HCEC-DM

Proteomic analysis showed the downregulation of Prx's in FED-affected corneal endothelium. To investigate this difference, real-time PCR was performed to evaluate the mRNA level of Prx-2, the most abundant Prx protein in corneal endothelium, as identified by 2-D gel electrophoresis. The PCR analysis was performed by using previously optimized primers and probes from Applied Biosystems. Four different pooled and nonpooled samples were used to compare the Prx-2 mRNA expression between FED and normal control samples. The real-time PCR showed a downregulation of Prx-2 mRNA levels in FED samples when normalized with the internal control

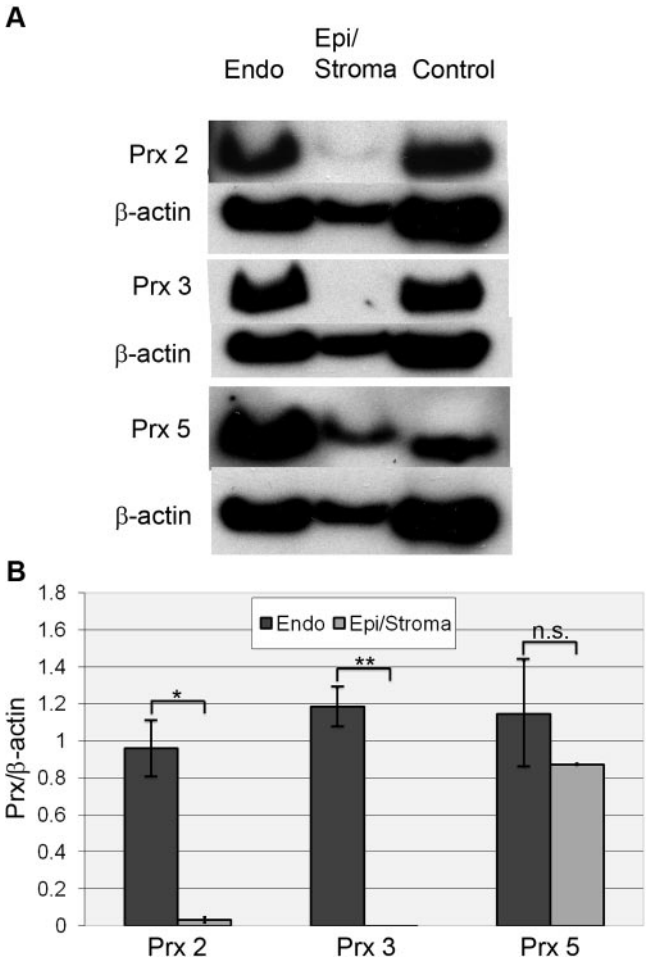

FIGURE 4. Western blot analysis of Prx isoform expression in normal corneal tissue. (**A**) Representative Western blot comparing the expression of Prx-2, −3, and −5 in normal human corneal endothelium (Endo) and epithelium/stroma (Epi/Stroma). Positive controls included LNCap cell lysate for Prx-2 and HeLa cell lysate for Prx-3 and −5. β-Actin was used for normalization of protein load. (**B**) Densitometric comparison of average Prx isoform expression from four independent samples (Table 1, samples 11–14). Bars: SEM. $^{*}P = 0.0034$; $^{**}P = 0.00062$. NS, not statistically significant ($P = 0.5$).

β2-MG (Fig. 5). The mean ± SEM relative expression of Prx-2 mRNA in FED group (0.32 ± 0.17) was significantly lower than that in normal subjects (1.03 ± 0.18; $P = 0.027$).

DISCUSSION

Although Prx proteins have been found to be ubiquitously expressed in human tissues, including skin, neuronal tissue, and blood cells,[18,20,21] this is the first study reporting the expression of Prx proteins in human cornea. Results of the proteomic analysis indicate that Prx-2, −3, −5, and −6 are expressed in normal corneal endothelium. Western blot studies confirmed the expression of Prx-2, −3, and −5 in these cells. The 2-D gel methodology showed that Prx-2 was the most abundantly expressed Prx protein in the endothelium, even though Prx-5 appeared as a more intense band in the Western blot analysis. Since the Western blot data are dependent on many factors, one of which is the sensitivity of the primary antibody, the spot intensity of the 2-D gels is a more accurate representation of the relative Prx levels in the sample. As indicated previously, expression of Prx-6 could not be verified by Western blot due to the lack of an antibody that worked sufficiently well. In the eye, Prx-6 expression has been noted in bovine iris stroma, lens, ciliary epithelium and its blood vessels, and retina.[22,23] In bovine cornea, Prx-6 was present in the epithelial layer, but not found in corneal endothelium.[23] The proteomic identification of Prx-6 in the current studies requires verification; however, the fact that Prx-6 was not detected in bovine corneal endothelium, but was detected in humans, may be due to species-related differences in protein expression or to differences in detection methods. It is also possible that Prx-1 or −4 is expressed in human corneal endothelium, but that they were not identified using our 2-D gel-based method.

In the present study, corneal stroma, and epithelium showed lower levels of Prx expression when compared to endothelium from the same donors. This is the first study to indicate that Prx-2 and −3 expression is significantly higher in human corneal endothelium than in the stroma and epithelium. Prx-5 was expressed in HCECs and to a lesser extent in epithelium/stroma; however, the difference in levels of this Prx isoform were not statistically significant. Selective expression of certain Prx isoforms in HCEC-DM, but not in epithelium/stroma, indicates distinct functional roles of antioxidant enzymes that reflect different physiologic activities of corneal cell types. It is possible that significantly higher expression of Prx-2 and −3 in corneal endothelium indicates selective vulnerability of specific corneal cell types to oxidative stress.

On the proteomic level we detected a significant reduction in Prx-2, −3, and −5 in FED endothelium. Tissues were used from age-matched normal donors to eliminate any age-related variation. The average differences in age between normal and FED pooled samples were within a decade of each other. The normal donors were matched by sex to patients with FED. For studies comparing protein expression in normal and FED endothelium, extracts from FED and normal donors were pooled to eliminate individual variations that might skew the results. One of the limitations of our study is that some samples contained an unequal number of pooled corneas between FED and normal samples. Since the overall endothelial cell count was much lower in FED samples, for the most part, more tissue was required to be pooled for FED samples. Two different semiquantitative methods were used to compare the relative expression of Prx isoforms. Both the software-based 2-D gel analysis and the Western blot analysis demonstrated a significant reduction in the expression of Prx-2, −3, and −5 in FED corneal endothelium compared with age and sex-matched normal specimens. Proteomic analysis comparing the normal and FED endothelial extracts revealed several differences in relative protein expression patterns, the significance of which should be further investigated. The fact that the relative expression of

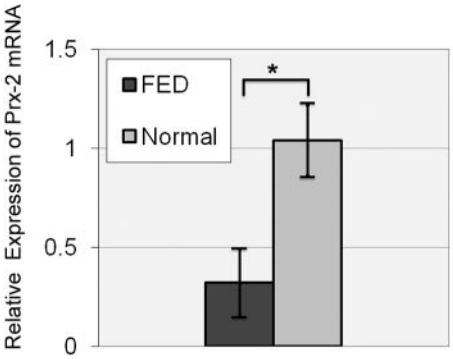

FIGURE 5. Real-time PCR analysis of Prx-2 isolated from normal and FED endothelium. Mean relative expression of Prx-2 messenger RNA (mRNA) in normal subjects and in patients with FED. Bars, SEM. $^{*}P = 0.027$.

SOD-1, another antioxidant enzyme, as well as the intermediate filament protein, vimentin, did not differ significantly between the FED and normal tissue strongly indicates that the reduction in expression of the Prx isoforms is specific and not the result of a general reduction in antioxidant or total protein expression.

Proteomic analysis of normal endothelium demonstrated that Prx-2 was the most abundant Prx isoform and thus of potential greatest significance at the functional level. To corroborate the decrease in Prx-2 levels in FED, we compared its expression at the gene level between normal and FED samples. The finding that levels of Prx-2 mRNA were significantly decreased in FED samples, further substantiates the proteomic data and indicates that the source of the differences detected by the proteomic analysis, at least for Prx-2, stem from decreased gene transcription.

Prx proteins have various subcellular locations, reflecting their multifunctional isoform diversity. Prx-2 is mainly a cytosolic protein that inhibits release of cytochrome *c* from mitochondria to cytosol and blocks hydrogen peroxide–induced apoptosis upstream of the site of Bcl-2 action.[24] In addition, activation of NF-κB induced by hydrogen peroxide is blocked by Prx-2, indicating its role in gene transcription regulation in response to reduction/oxidation status.[25,26] Because NF-κB has been implicated in regulation of corneal endothelial cell apoptosis in response to ROS, the potential role of Prx-2 as an endogenous inhibitor of NF-κB is particularly pertinent to HCEC physiology.[27] Prx-3 (MER 5, SP-22, and AOP-1) is a mitochondrion-specific peroxidase that uses mitochondrial thioredoxin-2 as an electron donor and provides primary antioxidant defense of the mitochondrial respiratory chain.[26] Underexpression of Prx-3 has been shown to exacerbate mitochondrial macromolecule damage via membrane potential collapse, cytochrome *c* release, and caspase activation.[28] Similar to our findings, Prx-3 has also been noted to be under-expressed in Alzheimer's disease (AD) and Down's syndrome (DS), disorders in which ROS-induced apoptosis accounts for the neuronal cell loss.[29,30] It has been postulated that the instability of Prx-3 in the neurodegenerative disorders accounts for the cells' susceptibility to oxidative stress. Prx-5 has been localized to the mitochondria, peroxisomes, and cell nucleus. Prx-5 also has a strong antiapoptotic function and prevents intracellular ROS production via a p53-dependent pathway.[17,31,32]

For future studies, it is important to correlate the downregulation of the Prx isoforms with apoptosis-related proteins, such NF-κB, caspase, and proteins involved in the p53-dependant pathways, as well as to substantiate further the role of Prx under-expression in the apoptotic cell death seen in FED endothelium. Since FED has a notable female preponderance, it is also important to explore Prx expression differences between the sexes. Also, because FED is for the most part a disease of the older population (>50 years of age), the changes in antioxidant expression between young and old donors may be of significance. Whether there is a variation in Prx expression between male and female sex and young and older donors requires further investigation. Furthermore, the downregulation of antioxidants in FED endothelium should be correlated with their upstream regulators, since Prx-2 underexpression is seen on both the RNA and protein levels.

Oxidative damage via generation of ROS can lead to corneal endothelial cell apoptosis and has been implicated in the pathogenesis of FED.[12,13] Antioxidant enzymes are critical for regulating intracellular levels of ROS and averting the deleterious effects associated with oxidative damage. Prx proteins constitute a potent antioxidant defense system by neutralizing ROS. The significant decrease in Prx levels in FED-affected cells may represent an alteration in the functioning of mechanisms required to combat oxidative stress related to the pathogenesis of this disease.

Acknowledgments

The authors thank all the Massachusetts Eye and Ear cornea surgeons, Peter Rapoza and Jonathan Talamo, and Roswell Pfister (The Eye Research Foundation, Birmingham, AL) for donating FED corneal specimens; Ann M. Bajart and Thomas Buckley of the New England Tissue Bank for donating normal corneal tissue; Sandra Spurr-Michaud for help with real-time PCR; and James Zieske for critical reading of the manuscript.

References

1. Darlington JK, Adrean SD, Schwab IR. Trends of penetrating keratoplasty in the United States from 1980 to 2004. *Ophthalmology*. 2006;113:2171–2175.
2. Wilson SE, Bourne WM. Fuchs' dystrophy. *Cornea*. 1988;7:2–18.
3. Laing RA, Leibowitz HM, Oak SS, Chang R, Berrospi AR, Theodore J. Endothelial mosaic in Fuchs' dystrophy: a qualitative evaluation with the specular microscope. *Arch Ophthalmol*. 1981;99:80–83.
4. Bahn CF, Falls HF, Varley GA, Meyer RF, Edelhauser HF, Bourne WM. Classification of corneal endothelial disorders based on neural crest origin. *Ophthalmology*. 1984;91:558–563.
5. Levy SG, Moss J, Sawada H, Dopping-Hepenstal PJ, McCartney AC. The composition of wide-spaced collagen in normal and diseased Descemet's membrane. *Curr Eye Res*. 1996;15:45–52.
6. Gottsch JD, Sundin OH, Liu SH, et al. Inheritance of a novel COL8A2 mutation defines a distinct early-onset subtype of Fuchs corneal dystrophy. *Invest Ophthalmol Vis Sci*. 2005;46:1934–1939.
7. McCartney MD, Robertson DP, Wood TO, McLaughlin BJ. ATPase pump site density in human dysfunctional corneal endothelium. *Invest Ophthalmol Vis Sci*. 1987;28:1955–1962.
8. Szentmary N, Szende B, Suveges I. Epithelial cell, keratocyte, and endothelial cell apoptosis in Fuchs' dystrophy and in pseudophakic bullous keratopathy. *Eur J Ophthalmol*. 2005;15:17–22.
9. Li QJ, Ashraf MF, Shen DF, et al. The role of apoptosis in the pathogenesis of Fuchs endothelial dystrophy of the cornea. *Arch Ophthalmol*. 2001;119:1597–1604.
10. Borderie VM, Baudrimont M, Vallee A, Ereau TL, Gray F, Laroche L. Corneal endothelial cell apoptosis in patients with Fuchs' dystrophy. *Invest Ophthalmol Vis Sci*. 2000;41:2501–2505.
11. Mullins RF, Russell SR, Anderson DH, Hageman GS. Drusen associated with aging and age-related macular degeneration contain proteins common to extracellular deposits associated with atherosclerosis, elastosis, amyloidosis, and dense deposit disease. *FASEB J*. 2000;14:835–846.
12. Wang Z, Handa JT, Green WR, Stark WJ, Weinberg RS, Jun AS. Advanced glycation end products and receptors in Fuchs' dystrophy corneas undergoing Descemet's stripping with endothelial keratoplasty. *Ophthalmology*. 2007;114:1453–1460.
13. Buddi R, Lin B, Atilano SR, Zorapapel NC, Kenney MC, Brown DJ. Evidence of oxidative stress in human corneal diseases. *J Histochem Cytochem*. 2002;50:341–351.
14. Gottsch JD, Bowers AL, Margulies EH, et al. Serial analysis of gene expression in the corneal endothelium of Fuchs' dystrophy. *Invest Ophthalmol Vis Sci*. 2003;44:594–599.
15. Jurkunas UV, Bitar MS, Rawe I, Harris DL, Colby K, Joyce NC. Increased clusterin expression in Fuchs' endothelial dystrophy. *Invest Ophthalmol Vis Sci.* 2008;49:2946–2955.
16. Rhee SG, Kim KH, Chae HZ, et al. Antioxidant defense mechanisms: a new thiol-specific antioxidant enzyme. *Ann N Y Acad Sci*. 1994;738:86–92.
17. Chae HZ, Robison K, Poole LB, Church G, Storz G, Rhee SG. Cloning and sequencing of thiol-specific antioxidant from mammalian brain: alkyl hydroperoxide reductase and thiol-specific antioxidant define a large family of antioxidant enzymes. *Proc Natl Acad Sci USA*. 1994;91:7017–7021.
18. Lee SC, Chae HZ, Lee JE, et al. Peroxiredoxin is ubiquitously expressed in rat skin: isotype-specific expression in the epidermis and hair follicle. *J Invest Dermatol*. 2000;115:1108–1114.

19. Zhu C, Joyce NC. Proliferative response of corneal endothelial cells from young and older donors. *Invest Ophthalmol Vis Sci*. 2004;45:1743–1751.
20. Lee TH, Kim SU, Yu SL, et al. Peroxiredoxin II is essential for sustaining life span of erythrocytes in mice. *Blood*. 2003;101: 5033–5038.
21. Sarafian TA, Verity MA, Vinters HV, et al. Differential expression of peroxiredoxin subtypes in human brain cell types. *J Neurosci Res*. 1999;56:206–212.
22. Peshenko IV, Singh AK, Shichi H. Bovine eye 1-Cys peroxiredoxin: expression in E. coli and antioxidant properties. *J Ocul Pharmacol Ther*. 2001;17:93–99.
23. Singh AK, Shichi H. Peroxiredoxin in bovine ocular tissues: immunohistochemical localization and in situ hybridization. *J Ocul Pharmacol Ther*. 2001;17:279–286.
24. Zhang P, Liu B, Kang SW, Seo MS, Rhee SG, Obeid LM. Thioredoxin peroxidase is a novel inhibitor of apoptosis with a mechanism distinct from that of Bcl-2. *J Biol Chem*. 1997;272:30615–30618.
25. Kang SW, Chae HZ, Seo MS, Kim K, Baines IC, Rhee SG. Mammalian peroxiredoxin isoforms can reduce hydrogen peroxide generated in response to growth factors and tumor necrosis factor-alpha. *J Biol Chem*. 1998;273:6297–6302.
26. Watabe S, Hiroi T, Yamamoto Y, et al. SP-22 is a thioredoxin-dependent peroxide reductase in mitochondria. *Eur J Biochem*. 1997;249:52–60.
27. Cho KS, Lee EH, Choi JS, Joo CK. Reactive oxygen species-induced apoptosis and necrosis in bovine corneal endothelial cells. *Invest Ophthalmol Vis Sci*. 1999;40:911–919.
28. Chang TS, Cho CS, Park S, Yu S, Kang SW, Rhee SG. Peroxiredoxin III, a mitochondrion-specific peroxidase, regulates apoptotic signaling by mitochondria. *J Biol Chem*. 2004;279:41975–41984.
29. Krapfenbauer K, Engidawork E, Cairns N, Fountoulakis M, Lubec G. Aberrant expression of peroxiredoxin subtypes in neurodegenerative disorders. *Brain Res*. 2003;967:152–160.
30. Kim SH, Fountoulakis M, Cairns N, Lubec G. Protein levels of human peroxiredoxin subtypes in brains of patients with Alzheimer's disease and Down syndrome. *J Neural Transm Suppl.* 2001(61);223–235.
31. Zhou Y, Kok KH, Chun AC, et al. Mouse peroxiredoxin V is a thioredoxin peroxidase that inhibits p53-induced apoptosis. *Biochem Biophys Res Commun*. 2000;268:921–927.
32. Chae HZ, Kim IH, Kim K, Rhee SG. Cloning, sequencing, and mutation of thiol-specific antioxidant gene of Saccharomyces cerevisiae. *J Biol Chem*. 1993;268:16815–16821.